2010 21st International Lightning Detection Conference
19 – 20 April • Orlando, Florida, USA
3rd International Lightning Meteorology Conference
21 – 22 April • Orlando, Florida, USA

Location Accuracy Improvements using Propagation Corrections: A Case Study of the U.S. National Lightning Detection Network

K. L. Cummins[1,2], M.J. Murphy[1], J. A. Cramer[1], W. Scheftic[2], N. Demetriades[1], A. Nag[3]
[1]Vaisala Inc. Tucson, Arizona
[2]University of Arizona, Tucson Arizona
[3]University of Florida, Gainesville, Florida

1. INTRODUCTION

A number of applications that employ information from Lightning Locating Systems (LLSs) require accurate estimates of the ground-strike location of return strokes in Cloud-to-Ground (CG) flashes. A study by Schulz and Diendorfer (2000) has shown that the primary factors limiting accurate geo-location of these strokes are (1) the delay of arrival-time of the return-stroke radiation field produced by variations in terrain elevation, and (2) frequency-dependent delay and attenuation of the ground-wave radiation field produced by propagation over finite-conductivity soil. It has been found that both of these propagation effects can be addressed by applying location-specific corrections to the arrival times measured by LLS sensors.

This paper provides an overview of Vaisala's propagation correction methodology as applied to the NLDN, and includes performance-related analyses using both natural and rocket-triggered lightning (RTL) from 2008-9. Both theoretical and experimental analyses indicate that these corrections produce approximately a factor-of-two improvement in location accuracy, with typical median values in the range of 200 m. A preliminary unpublished study of corrected and uncorrected location accuracy for the NLDN was carried out by one of the authors (A. Nag) using RTL data from the summers of 2003-4. Results from this study are consistent with the findings reported by Nag, and are from a more-recent time period. Networks with closer-spaced sensors (<~150 km) typically experience less improvement from the use of propagation corrections, but they also normally start out with RMS timing errors well under one μs.

2. GEO-LOCATION OF CG LIGHTNING STROKES

Modern LLSs that focus on the detection and location of CG lightning generally employ a network of broadband (~1 kHz to 400 kHz) sensors that identify electric and/or magnetic fields waveforms produced by return strokes. The fast-rising "onset" of these fields produces a distinct waveform feature that can provide an accurate time of arrival, and the ratio of the peak field values measured by a pair of north-south and east-west magnetic field antennas can provide an accurate direction of arrival. The most general location method is referred to as the "IMproved Accuracy through Combined Technology" (IMPACT) algorithm that simultaneous uses both the directional (azimuth) and arrival-time information (Cummins and Murphy, 2009). This algorithm produces three estimated parameters -- latitude, longitude, and discharge time. Thus as few as two combined IMPACT sensors provide redundant information which allows for an optimized estimate of location. The IMPACT algorithm can utilize information from any combination of direction finding (DF), time-of-arrival (TOA), or combined (DF/TOA) sensors. Figure 1 shows a typical lightning stroke in Florida that was detected by five sensors in the NLDN – three IMPACT and two time-of-arrival sensors. The direction (azimuth) measurements are shown as straight-line vectors, and "range circles" centered on each sensor represent the time-of-arrival measurements in the form of the propagation time from the discharge to each sensor. The IMPACT systems are now the most common LLS configuration, given the small number of sensors required to produce a location, and the use of calibrated magnetic field measurements for peak-current estimation.

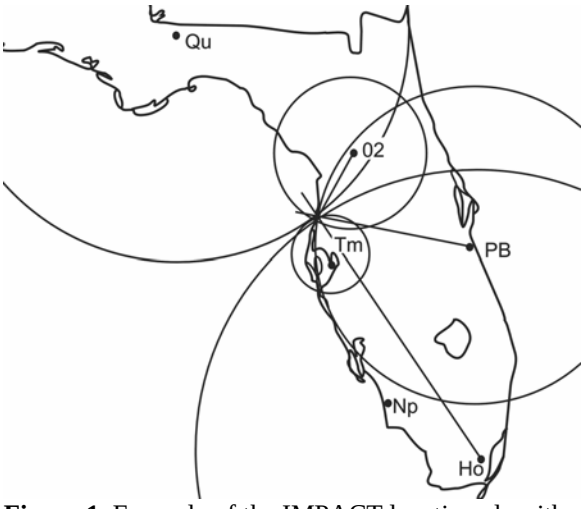

Figure 1. Example of the IMPACT location algorithm using three time-of-arrival sensors and two IMPACT sensors.

Direction finding and time-of-arrival contribute differently to location accuracy, depending on the geometry of the LLS. Properly calibrated DF systems that employ an optimization-based location algorithm are able to locate CG strokes with an accuracy better than 500 m for sensor baseline distances of less than 50 km (Maier and Wilson, 1996). However, location errors for DF systems are directly proportional to baseline distances, so a network composed of DF sensors with 200-300 km baselines can only provide location accuracy in the range of 2-4 km at best (Cummins et al., 1998a). However, to first order, the location accuracy in the interior of a time-or-arrival based LLS is independent of sensor baseline distances, and is directly proportional to the error in the arrival-time measurements. The mechanism for the small relative error in the interior of such a network is illustrated in Figure 2. The stroke occurring inside the network is located by three sensors (A,B,C), represented by the intersection of two hyperbolas (solid lines). The thinner lines placed symmetrically along the solid lines represent hyperbolas of fixed timing deviation (error) from the "true" value. For this stroke, the intersection of these lines forms a small, solid diamond that is nearly square, representing small location error. In the ideal case where timing error is independent of propagation distance, the separation of the error lines in the interior of the network does not increase with increasing sensor baseline distances. The stroke occurring outside the network has a very elongated region of location uncertainty, resulting from both the more parallel intersection of the hyperbolas and the diverging nature of the thin lines that represent the effect of timing error.

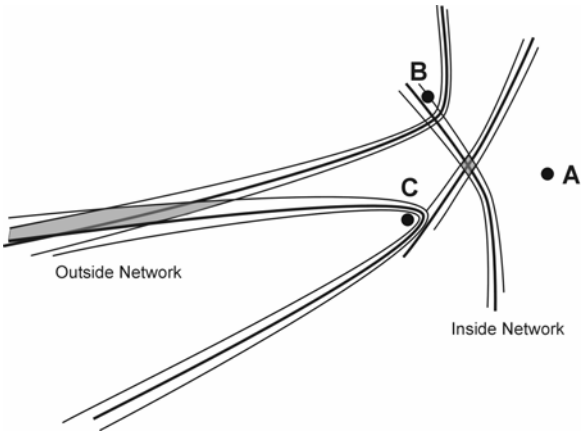

Figure 2. Illustration of differences in TOA-based location accuracy for sources located inside and outside a 3-sensor network (locations A-C).

When direction-finding and time-of-arrival measurements are combined, the optimization process naturally ends up being driven by whichever set of measurements best constrains the discharge location. In the interior of a short-baseline network (e.g. 50 km), both angle and time may end up being weighted equally, but given the long baseline distances in the NLDN (300-350 km), errors in the time-of-arrival measurement are the dominant factor determining location accuracy. The NLDN sensors have been shown to have a nominal time-of-arrival error of 1.5 μs RMS, which leads to an estimated median location error of 500 meters or better (Cummins and Murphy, 2009), which has been verified in numerous studies (Nag et al., 2008, Biagi et al., 2007, Cummins et al., 2006, Jerauld et al., 2005)

The time-of-arrival error (and therefore the location error) is principally determined by the propagation of lightning electromagnetic fields over mountainous and finite-conducting terrain (Murphy and Pifer, 1998; Honma et al., 1998; Schulz and Diendorfer, 2000). It has been found that both of these propagation effects can be addressed by applying location-specific corrections to the arrival times measured by LLS sensors. This has led Vaisala to develop a method to estimate these so-called propagation corrections, as a function of azimuth and range from each sensor, using high-resolution digital elevation terrain data and very large lightning datasets. These corrections are applied during a "second pass" of location processing once a "preliminary" location is calculated. The preliminary calculation provides the means to index into the propagation correction datasets for each sensor.

3. DATA AND ANALYSIS METHODS

The U.S. National Lightning Detection Network (NLDN) detects CG lightning flashes and strokes, as well as a small percentage of cloud events (Cummins et al. 2006; Orville 2008; Cummins and Murphy 2009). The NLDN reports the time, location, estimated peak current and waveform parameters for 90-95 percent of all CG flashes within ~250 km of the continental U.S, with degrading performance at greater distances. It also reports 70-80 percent of all return strokes. Each stroke report is accompanied by a set of location quality parameters described in detail in Cummins et al. (1998a,b). In brief, this includes the value of a normalized chi-square (χ^2) error function at the optimum location and the size and orientation of the semi-major axis (SMA) of a confidence ellipse that describes the accuracy of the location. The value of χ^2 is a normalized measure of the "agreement" among all reporting sensors. Ideally, the distribution of χ^2 values has a mean and standard deviation of unity, but values between 0 and 3 are considered to be "good," and values between 3 and 10 are "acceptable." The semi-major and semi-minor axes of the confidence ellipse

characterize the dimensions of a region that should contain the actual stroke location (to within a given probability), and are based on a two-dimensional Gaussian distribution of location errors that are inferred from known measurement errors and the geometry of the sensor locations.

In this study, propagation time corrections for each NLDN sensor were derived using the following general procedure. First, a digital elevation model of the U.S. was used to calculate an initial set of propagation corrections for each sensor based on path elongation only. Next, the continental U.S. was divided into a fine-mesh set of grid regions, and each hour of lightning data for the thunderstorm seasons of 2008 and 2009 was inspected in order to determine which hours could be used to provide (fairly) uniform coverage of lightning throughout the set of grid regions. These data were then reprocessed for the selected hours, and time deviations (arrival-time error relative to the "optimal" value estimated from all reporting sensors) for each sensor were calculated as a function of range and azimuth from the sensor. The deviations were then used to produce an initial correction (as a function of range and azimuth) to be applied during a next iteration of reprocessing. This procedure was repeated until the calculated corrections converged to stable values, and the residual errors no longer decreased. These final propagation corrections were then employed in all subsequent analyses. An example of the corrections for a representative sensor is provided in Figure 3. The arrival-time correction (in 10 μs units) is plotted using a heat-scale color map, and overlaid on 1000 ft. (~300 m) terrain isoclines. These corrections are slightly negative near the sensor (the black circle in the middle of the figure), and increase monotonically with increasing distance from the sensor. Note that the magnitude of the correction is dependent on azimuth, reflecting differing terrain and conductivity in different directions from the sensor.

In this work, the performance analyses focus on the location uncertainty in CG flash and stroke data obtained in 2008 and 2009. Estimates of arrival-time error and location error were determined both before and after applying propagation corrections. The arrival-time error was evaluated as follows. For each sensor, histograms of the arrival-time error for all strokes were produced. The mean and standard deviation of the arrival-time error was also calculated as a function of arrival angle and distance to the stroke location, in order to evaluate biases at different azimuths and ranges.

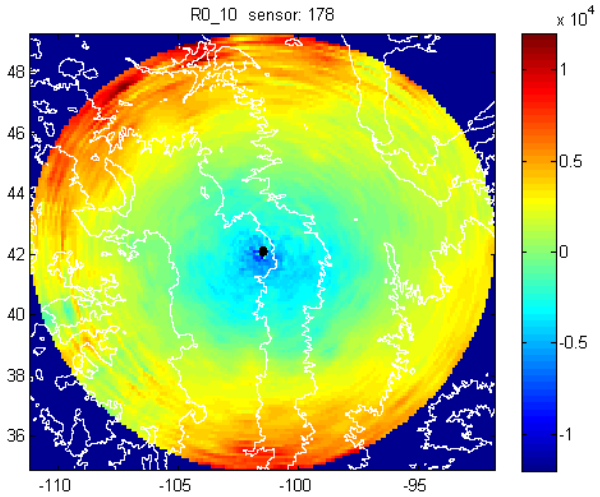

Figure 3. Thematic map of the propagation correction for a selected sensor. Corrections are computed within a radius of 800 km. The color scale goes from +/- 12 μs, increasing monotonically with range. The white contours are 1000 ft (~330 m) isoclines.

The location error was evaluated in two ways. Absolute location error was evaluated using rocket triggered lightning (RTL) measurements obtained in 2008-9 at the International Center for Lightning Research and Testing (ICLRT) at Camp Blanding, Florida. Relative location accuracy was determined in two other regions (Tennessee and south-central Arizona) using the following procedure:

1. Individual return stroke locations for the 72-hour period of June 18-20, 2009 were extracted for the two regions from the Vaisala database (uncorrected locations) and from the final corrected dataset. The specific rectangular regions were selected to encompass domains with large variations in elevation and soil electrical conductivity.
2. These stroke datasets were time-correlated with each other in order to produce two matched datasets.
3. Negative strokes in each dataset were grouped into flashes using the standard NLDN flash grouping algorithm (Cummins et al., 1998a). Note that this process resulted in small differences in some flashes, due to small differences in the locations of individual strokes.
4. The first stroke and the last stroke in each flash were selected as "reference strokes", and distances (position differences) between these strokes and all other strokes in the flash were tabulated.
5. Two position-difference histograms were produced for both the uncorrected and corrected datasets. One histogram includes distances of the second and third strokes relative to the first stroke. Based on studies of

multiple ground contacts in negative CG flashes (Rakov et al., 1994; Valine and Krider, 2002), roughly 1/3 of all negative CG flashes have two or more separate ground contacts, usually occurring for the second and/or third stroke in the flash. There are approximately 1.5 ground contacts per multi-stroke negative flash. Therefore, this first histogram is composed of two (approximately) equal-sized populations of "new ground contact" (NGC) strokes and "pre-existing channel" (PEC) strokes. The second histogram is for the location of strokes of order 5 and higher, relative to the last stroke in the flash. Clearly, these only occur for flashes with 6 or more strokes. Work by Rakov et al. (1994), recently confirmed by Stall et al. (2009) (and other studies), indicates that strokes of order 5 or higher remain in a pre-existing channel. Therefore this second histogram is strictly composed of position differences for PEC strokes, and therefore represents the random location error in the region.

4. RESULTS.

The following three subsections illustrate improvements in timing error, absolute location error, and relative location error resulting from applying propagation corrections to the NLDN sensor arrival-time measurements.

4.1. Arrival-time Error Analysis

As noted in Section 2, location errors in the interior of a long-baseline LLS (sensor separation distances of roughly 200 km and greater) are determined by the arrival-time measurement errors. In addition, the resulting location error is linearly related to the magnitude of the arrival-time error. Figure 4 illustrates the reduction in this error for a representative NLDN IMPACT sensor produced using the propagation correction procedure described in Section 3. The upper row shows the arrival-time error (deviation) for the operational (online) NLDN configuration. The upper center panel is a frequency histogram of time deviations, composed of over 350,000 observations. The RMS value in this image is the standard deviation of a best-fit normal distribution, trimmed to exclude extreme tails in the observed histogram. The upper left panel shows the distribution of these observations (blue histogram) as a function of azimuth (0-360 degrees from north), and the upper right panel shows the distribution of observations as a function of range (distance in km) from the sensor (blue histogram).

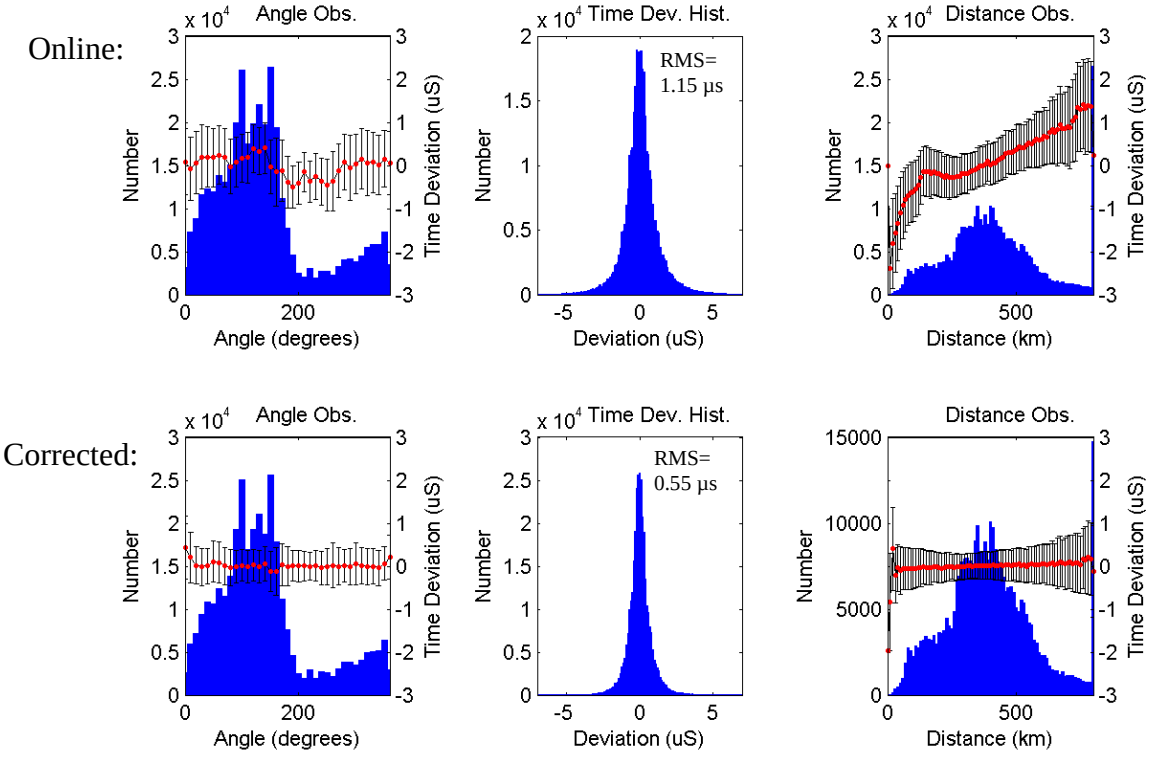

Figure 4 Arrival-time errors as a function of arrival-angle (clockwise from north) and range (distance) for a representative NLDN sensor. The upper row shows results before applying corrections; the lower row is after corrections.

Additionally, The arrival-time deviations are depicted in the left and right panels, with the population means in red, and the +/-1 standard deviation (RMS value) as error bars. It is clear from these upper panels that there are significant biases (non-zero mean) of the timing error as a function of both angle and range, with biases of +/- 1.5 μs as a function of range. The lower row shows the arrival-time error after applying propagation corrections. The RMS error was reduced by more than a factor of two (from 1.15 to 0.55), and the bias errors as a function of azimuth and range are essentially eliminated.

Figure 5 contains histograms of overall RMS timing error in our dataset for every sensor in the NLDN and the Canadian Lighting Detection Network (CLDN) (Orville et al, 2002). The red histogram shows the distribution of timing errors when no corrections are applied. The overall RMS error for all uncorrected sensors is 1.48 μs. The individual sensor RMS errors range from 0.6 to 2.6 μs. The blue histogram shows the distribution of timing errors after applying propagation corrections. The overall RMS value is reduced to 0.67 μs, and the range is from 0.2 to 1.4 μs. These population results also show more than a factor-of-two improvement in timing errors as a result of propagation corrections. Theoretically, this will result in at least a factor-of-two improvement in location accuracy.

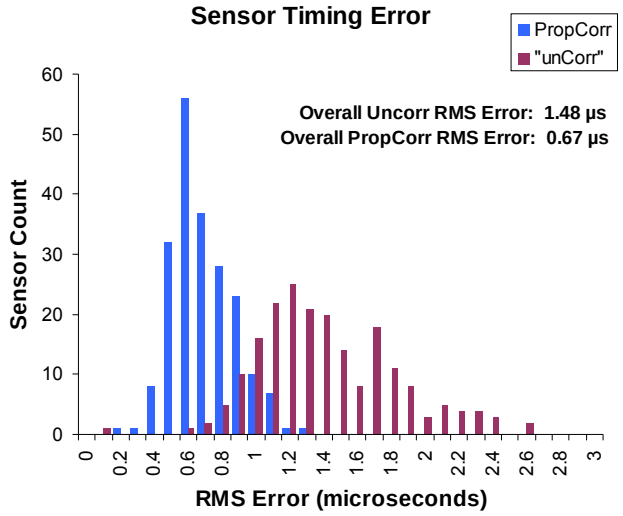

Figure 5. RMS timing error for all NALDN sensors before propagation corrections (red histogram) and after applying propagation corrections (blue histogram).

4.2. Validation using Rocket Triggered Lightning

As noted in Section 3, rocket triggered lightning (RTL) provides a means to determine the absolute location accuracy of a lighting locating system (see for example Jerauld et al., 2005). During 2008 and 2009, there were 25 triggered flashes with 111 return strokes. The "Online" NLDN reported 87 strokes (78%) in 24 of these flashes (96%), and the propagation-corrected NLDN reported 90 strokes (81%) in all 25 of these flashes (100%). The remaining analysis here is limited to a presentation of location accuracy.

Figure 6 contains histograms of the location error for the online NLDN configuration (red) and the propagation corrected configuration (blue). Most of the corrected errors are below 300 m, with scattered errors out to 2.3 km. The online configuration has more broadly spread errors, with many values extending out to 600 m. The mean errors are similar for the two conditions, but the median values for the Online condition are 50% larger. The mean values are principally determined by the "tail" of these distributions above 1 km. These tails are produced by less than 7% of the data, and are associated with locations that are known to have large semi-major axis values.

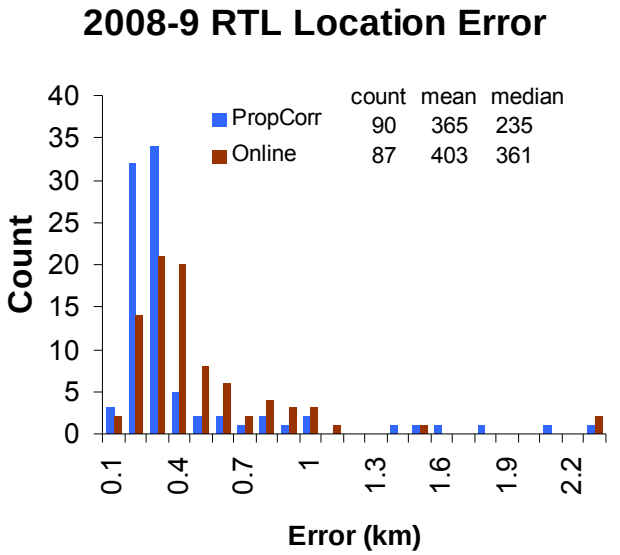

Figure 6. Absolute location error relative to the triggering site. The red histogram shows the error before applying corrections, and the blue histogram shows the error after applying propagation corrections.

The mean and median error values for the online configuration (403 and 361 m, respectively) are better than values obtained in 2003 by Jerauld et al. (2005) (34 strokes; mean/median of 640/450 m). This is thought to be due to replacement of the last LPATS sensor in Florida by an IMPACT sensor later in 2003 (resulting in a homogenous network configuration), and small refinements in the site error (angle) corrections. Both Jerauld et al. (2005) and the current study found that location accuracy of the online NLDN data was better than the 500 m median value put forth by Vaisala, possibly because of the flat terrain and rather uniform electrical conductivity in the Florida peninsula. The median value obtained

using propagation corrections is more than a factor of two better than Vaisala's stated accuracy.

The spatial distribution of the location errors is shown in Figure 7. Locations for the online configuration are shown in red, and for the propagation-corrected configuration are shown in blue. The propagation corrected strokes cluster much closer to the triggering location (located at the origin of the plot), whereas the online strokes show more scatter and an offset to the west. Both configurations show some scattered strokes with a somewhat southwest-to-northeast orientation. All these strokes occurred in 2009, at times when critical sensors to the northwest or southeast were not operating. The Florida peninsula is prone to such sensitivity because there are no sensors to the east or the southwest.

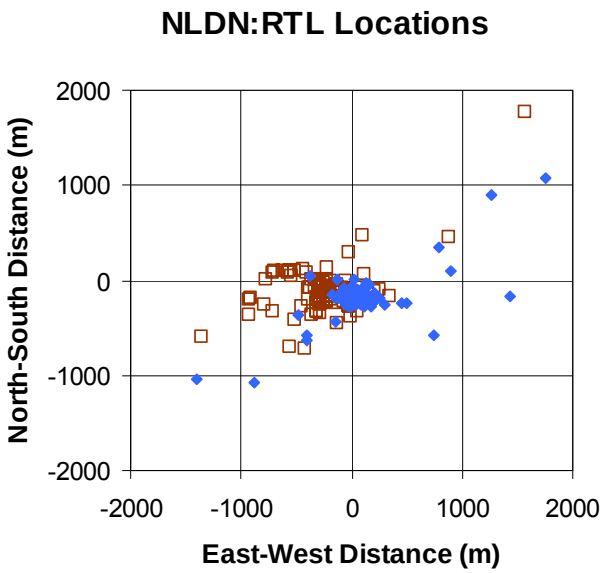

Figure 7. Scattergrams of location deviation from the triggering site (center location). The population of uncorrected locations (red) show more scatter and offset than the propagation-corrected locations (blue points).

4.3. Validation using CG Flash Characteristics

Since RTL sites are not available in other locations in the U.S., a less-direct method was employed to assess location accuracy in other areas. Relative location accuracy was evaluated in several regions; we show results from two representative regions (central Arizona and Tennessee), using the procedure described in Section 3.

Relative location accuracy is a measure of the location difference between two return strokes. Since both of these locations are subject to random errors, the location difference will generally be larger then the error associated with either of the two strokes. If one assumes that the random location errors for both strokes are uncorrelated but statistically equal, then the large-population distribution of the distance difference will be larger than the individual stroke location error by $\sqrt{2}$ (41% too large). This type of analysis was first carried out by Biagi et al. (2007).

Results for Arizona are shown in Figure 8. The upper panel shows the distribution of distance difference for 80+ strokes (of order 5 and above), relative to the last stroke in the flash. This distribution is used to characterize the location differences for strokes that share the same pre-existing channel (PEC) to ground (see Section 3). Results for the online (red) configuration show a broader range of distance differences than with the propagation corrected (blue) configuration. The mean and median values for the online configuration (0.69 and 0.39 km, respectively) are slightly smaller than those obtained by Stall et al. (2009) in the Tucson region (0.9 and 0.7 km, respectively) using video-confirmed same-channel strokes. This is likely because the Tucson study was at the southern edge of the NLDN, whereas the current study was carried out in central Arizona, in the interior of the NLDN where the location accuracy is expected to be somewhat better. Since the values are smaller than those found by Stall et al., we have confidence that the procedure for identifying same-channel strokes is statistically reliable. Taking into consideration the $\sqrt{2}$ factor, the expected random location error in this region changed from 276 m to 191 m as a result of propagation corrections.

The lower panel of Figure 8 shows the distribution of distance differences for 470+ strokes (of order 2 and 3), relative to the first stroke of the flash. The mean, median, and standard deviation (S.D.) values are almost identical for uncorrected and corrected data sets (red and blue, respectively). These values are all much larger than for the PEC condition in the upper panel, since a large fraction of these stokes created a new ground contact (NGC), producing real differences in stroke location. The mean and median values are smaller than found by Stall et. al. (2.3 and 2.1, respectively), but this is expected because we have no way to eliminate the fraction (roughly half) of these strokes that did remain in an existing channel.

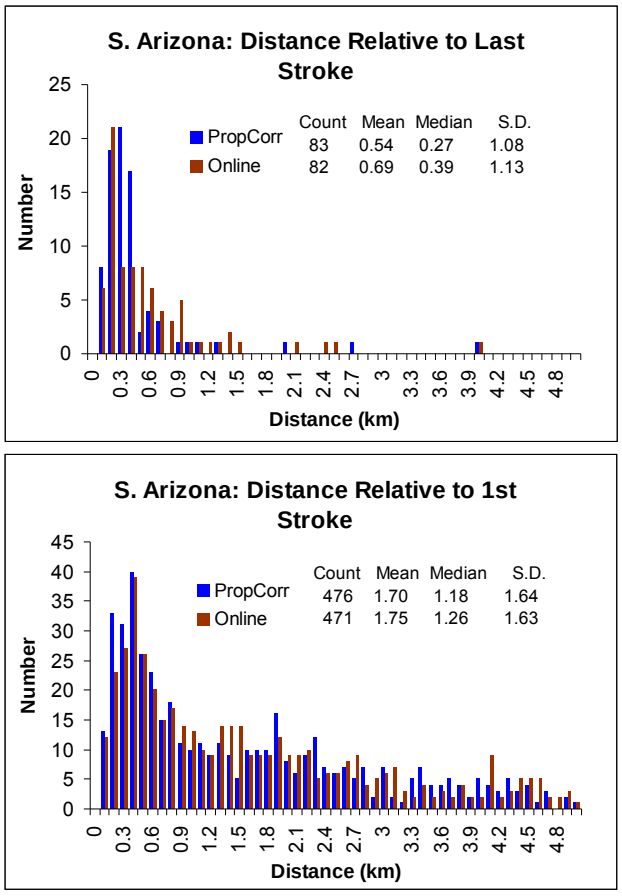

Figure 8. Separation distances for un-corrected and propagation-corrected strokes. See text for details.

The results of this same analysis in the Tennessee area are shown in Figure 9. The median values for the PEC condition (upper panel) are almost identical to what was found in Arizona, with 5 times as many observations. The mean and S.D. values are much larger, due to a larger fraction of location differences greater than 1.5 km. We cannot say whether these are true location errors, or contamination of the dataset by a few NGC strokes. Irrespective, the expected random error in this region changed from 276 m to 198 m as a result of the corrections.

The NGC results in the lower panel of Figure 9 are quite similar to what was found in Arizona, although the median values are slightly lower and the S.D. values are slightly higher. As in Arizona, there is little difference in NGC location differences for the online and propagation-corrected data sets, indicating that the location error is dominated by true differences in stroke locations.

The results in Figures 8 and 9 indicate that the median random location error in both central Arizona and Tennessee is less than 200 m, when propagation corrections are applied. The true location error includes the random location error discussed here, plus any residual bias error that is an offset of the average location in a specific region (such as shown in Figure 7). Thus the true median location error in these regions is probably a bit larger. However, it is unlikely that the error is larger than the 235 m median value found for rocket triggered lightning (Figure 6), since the ICLRT is located at the edge of the NLDN network, where location errors start to increase.

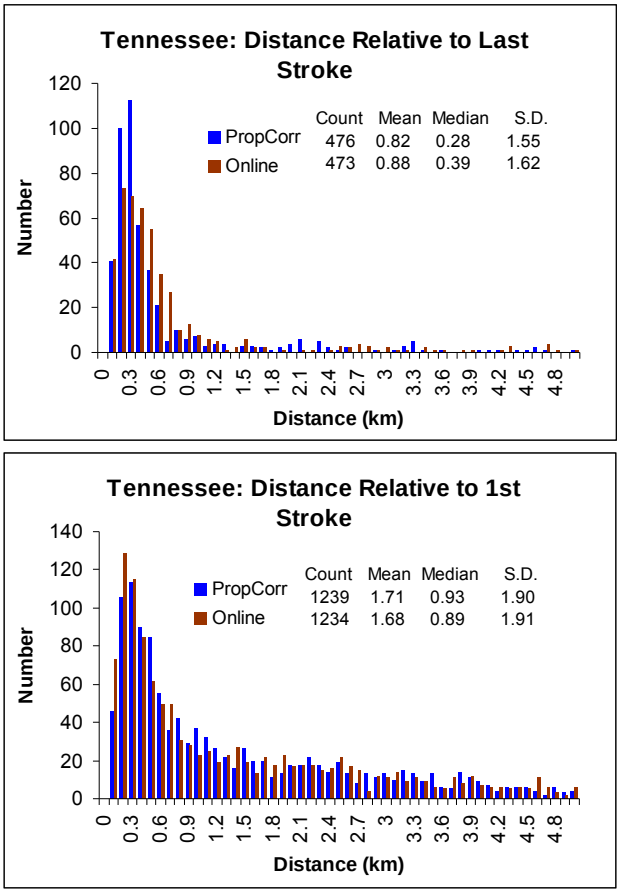

Figure 9. Separation distances for un-corrected and propagation-corrected strokes. See text for details.

5. SUMMARY

This paper provides an overview of the propagation correction methodology as applied to the NLDN, and includes performance-related analyses using both natural and rocket-triggered lightning. The correction process reduces the error in the arrival-time measurement for widely-spaced sensors (~300-400 km) from approximately 1.5 μs RMS to less 0.7 μs RMS. This results in approximately a factor-of-two improvement in location accuracy, with typical median values in the range of 200-235 m. Networks with closer-spaced sensors (<~150 km) will generally experience less improvement from the use of propagation

corrections, but they typically have RMS timing errors well under one μs RMS initially.

Over the next several months, the propagation corrections will be refined and evaluated in more regions. Vaisala expects to put these corrections into real-time use in late 2010 or early 2011.

Acknowledgment

The authors thank Wolfgang Schulz for his contributions to the analysis and implementation of propagation corrections, including his early work in Austria. We also thank V.A. Rakov and M.A. Uman for providing access to the rocket triggered lighting data from the International Center for Lightning Research and Testing (ICLRT). Finally, we thank C. Biagi for preparing the ICLRT data and for providing support during its analysis.

REFERENCES

Biagi C.J., K.L. Cummins, K.E. Kehoe, E.P. Krider, (2007) "NLDN Performance in Southern Arizona, Texas and Oklahoma in 2003-2004", *J. Geophys. Res.*, **112**, D05208, doi:1029/2006JD007341.

Cummins K and Murphy M. (2009), An Overview of Lightning Locating Systems: History, Techniques, and Data Uses, With an In-Depth Look at the U.S. NLDN (2009 - invited paper), *IEEE Transactions on Electromagnetic Compatibility*, Vol. 51 (3), pp. 499-518, August 2009.

—, J.A. Cramer, C.J. Biagi, E.P. Krider, J. Jerauld, M.A. Uman, and V.A. Rakov (2006) The U.S. National Lightning Detection Network: Post-upgrade status. *Preprints, 2nd Conference on Meteorological Applications of Lightning Data*, January 29-February 2, Atlanta, Georgia, American Meteorological Society, 9 pp.

—, EA Bardo, Hiscox WL, Pyle RB, Pifer AE, Murphy MJ (1998a), A combined TOA/MDF technology upgrade of the US national lightning detection network. *J. Geophys. Res*., 103 (08): 9035-9044, April 1998.

—, E.P Krider, Malone, MD (1998b), The U.S. national lightning detection network™ and applications of cloud-to-ground lightning data by electric power utilities. *IEEE Transactions on Electromagnetic Compatibility*, **40** 4, November 1998.

—, and M.J. Murphy (2009), An overview of lightning locating systems: History, techniques, and data uses, with an in-depth look at the U.S. NLDN. *IEEE Transactions on Electromagnetic Compatability*, **51**, 3, 499-518.

Honma N., F. Suzuki, Y. Miyake, M. Ishii, S. Hidayat, (1998), "Propagation Effect on the Field Waveforms in Relation to TOA Technique in Lightning Location", *J. Geophys. Res.*, **103**, pp. 14141-14146.

Jerauld, J., V.A. Rakov, M.A. Uman, K.J. Rambo, D.M. Jordan, K.L. Cummins, and J.A. Cramer, (2005), An evaluation of the performance characteristics of the U.S. National Lightning Detection Network in Florida using rocket-triggered lightning. *J. Geophys Res.*, **110**, doi:10.1029/2005JD005924.

Maier M.W. and M.B. Wilson, (1996), Accuracy of the NLDN real-time data service at Cape Canaveral, Florida, *Preprints, International Lightning Detection Conference*, November 6-8, Tucson, Arizona, Global Atmospherics, Inc., Tucson, 1996.

Murphy M.J., A.E. Pifer (1998), "Network Performance Improvements using Propagation Path Corrections," *Preprints, 1998 International Lightning Detection Conference*, Tucson, Arizona.

Nag, A., J. Jerauld, V.A. Rakov, M.A. Uman, K.J. Rambo, D.M. Jordan, B.A. DeCarlo, J. Howard, K.L. Cummins, and J.A. Cramer (2008), NLDN responses to rocket-triggered lightning at Camp Blanding, Florida, in 2004, 2005 and 2007, *29th International Conference on Lightning Protection*, paper no. 2–05, Uppsala, Sweden.

Orville, R.E., G.R. Huffines, W.R. Burrows, R.L. Holle, K.L. Cummins (2002), The north-American lightning detection network (NALDN) – First results: 1998-2000, *Monthly Weather Review*, Vol. 130, No. 8, August 2002.

—, (2008), Development of the National Lightning Detection Network", *Bulletin of the American Meteorological Soc*., vol. 89, no. 2, doi:10.1175/BAMS-89-2-180, Feb. 2008.

Rakov, V.A., M.A. Uman, R. Thottappillil, (1994), Review of lighting properties from electric field and TV observations, *J. Geophys. Res*, **99**, pp. 10,745-10,750.

Schulz W., G. Diendorfer (2000), Evaluation of a Lightning Location Algorithm using a Elevation Model, *Proceedings of the 25th International Conference on Lightning Protection*, Paper 2.3, Rhodes, Greece, 18-22 September.

Stall, C.A., K.L. Cummins, E.P. Krider, and J.A. Cramer (2009), Detecting multiple ground contacts in cloud-to-ground lightning flashes. *J. Atmos. Ocean. Tech.*, **11**, 2392-2402.

Valine, W. C. and E. P. Krider (2002) Statistics and characteristics of cloud-to-ground lightning with multiple ground contacts, *J. Geophys. Res*., 107, 4441, doi:10.1029/2001JD001360.